

# Structural and optical properties of Ta<sub>2</sub>O<sub>5</sub>:Eu<sup>3+</sup>: Mg<sup>2+</sup> or Ca<sup>2+</sup> phosphor prepared by molten salt method.

Naveen Verma<sup>1\*</sup>, Bernabe Mari<sup>2</sup>, Krishan Chander Singh<sup>1</sup>, Jitender Jindal<sup>1</sup>, Miguel Mollar<sup>2</sup>, Ravi Rana<sup>3</sup>, A. L. J. Pereira<sup>4</sup>, F. J. Manjón<sup>2</sup>

<sup>1</sup>Department of chemistry, Maharshi Dayanand University, Rohtak- 124001 – India

<sup>2</sup>Institut de Disseny per la Fabricació Automatitzada - Departament de Física Aplicada, Universitat Politècnica de València, Camí de Vera s/n, 46022 València, Spain

<sup>3</sup>Department of Chemistry, SGT University, Gurgaon, India

<sup>4</sup>Universitat Politècnica de València, 46022 València, Spain

Corresponding author\*: [vermanaveen17@gmail.com](mailto:vermanaveen17@gmail.com)

**Abstract.** Ta<sub>2</sub>O<sub>5</sub>:Eu<sup>3+</sup>: Mg<sup>2+</sup> or Ca<sup>2+</sup> phosphor materials were prepared by molten salt method using KCl as flux. The X-ray diffraction (XRD) patterns illustrated that the well crystallized Ta<sub>2</sub>O<sub>5</sub>:Eu<sup>3+</sup>: Mg<sup>2+</sup> or Ca<sup>2+</sup> were formed in the presence of flux under reduced temperature (800 °C) in contrast to conventional solid state method (1200-1500 °C). Scanning electron microscope (SEM) images indicate the achievement of well dispersed particles (hexagonal tablet and rod-like structures). Meanwhile, the photo-luminescent studies demonstrated that Ta<sub>2</sub>O<sub>5</sub> is an efficient host to sensitize europium red emissions. The addition of Mg<sup>2+</sup> or Ca<sup>2+</sup> as co-dopant enhanced the luminescent intensity of Ta<sub>2</sub>O<sub>5</sub>: Eu<sup>3+</sup> compound.

## INTRODUCTION

The applications of fluorescent materials (phosphor) are pervasive in day to day life, for example, in fluorescent dazzling lighting, PC screens, emerging LED based solid state lighting, family unit apparatus and so forth. [1-2]. The improvement of functional rare earth doped phosphors have prompted new applications in few fields, most outstandingly in fluorescent lights, cathode beam tube and lasers. [3-5]. In recent years, transparent wide band gap oxides have been doped mainly to tune desirable properties for optical and electrooptical applications [6]. In addition rare earth metals provide 4f<sup>n</sup> transitions showing high luminescence efficiency doped in several hosts lattices [7- 9] for solid state laser applications [10]. The tantalum (V) oxide (Ta<sub>2</sub>O<sub>5</sub>) has potential as a host material for new phosphors due to its low photon energy (100 –450 cm<sup>-1</sup>) [11]. Compared with host materials such as SiO<sub>2</sub> and other wide band gap oxides, Ta<sub>2</sub>O<sub>5</sub> provide opportunities to sensitize rare earth characteristic emissions. Therefore, improving the activity of Ta<sub>2</sub>O<sub>5</sub> through encapsulation of lanthanide ions has been developed [12-16].

Ta<sub>2</sub>O<sub>5</sub> has attracted much attention of numerous researchers due to its remarkable optical, catalytic, dielectric and chemical properties [17]. Optically active rare earth doped Ta<sub>2</sub>O<sub>5</sub> films have been synthesized for the purpose of developing compact sources and amplifiers for the telecommunication applications [18-19]. Also due to their higher transparency and extensive range, Ta<sub>2</sub>O<sub>5</sub> crystals offer the prospect of low loss optical waveguides [20]. In this section, we reported the preparation of Eu<sup>3+</sup> doped Ta<sub>2</sub>O<sub>5</sub> phosphor with different concentration of alkaline earth metal ions (Mg<sup>2+</sup> or Ca<sup>2+</sup>) as co-dopant by molten salt method and investigation of the optical and structural properties of the materials with the help of luminescence spectra, FESEM images and XRD patterns.

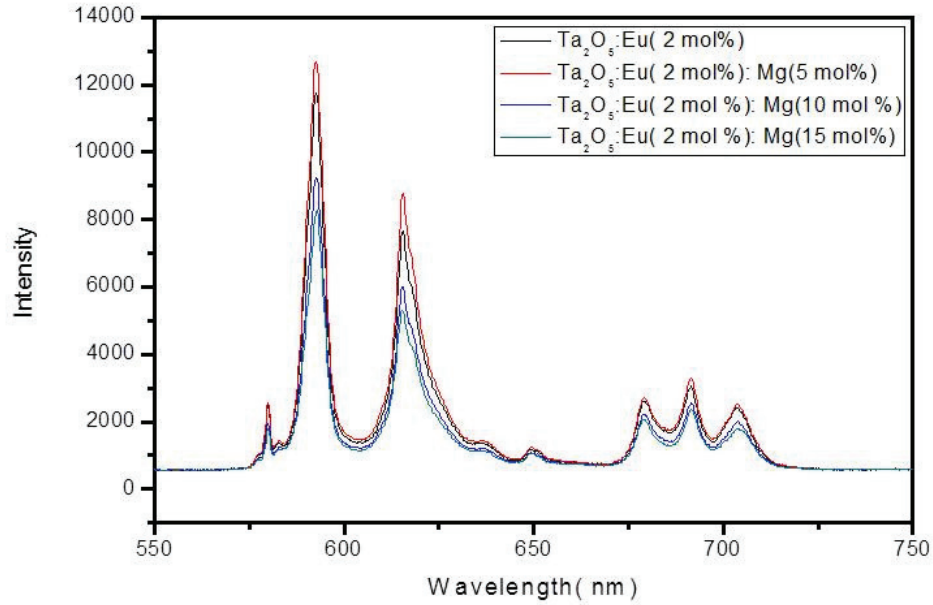
## EXPERIMENTAL

All the beginning materials like Ta<sub>2</sub>O<sub>5</sub>, Eu<sub>2</sub>O<sub>3</sub>, MgO, CaO and KCl were acquired from Sigma Aldrich and utilized as provided without further purification. The stoichiometric amount of different compositions were taken and ground sufficiently in an agate mortar. KCl was used as flux in the synthesis mixture. In the following step, the homogeneous mixture was transferred to a crucible and sintered at a temperature of 800°C for 2 hour in air. In the wake of cooling to room temperature in furnace, the mixed oxide phosphor powder was washed with distilled water five times so as to remove the molten salt totally. At last, the phosphor was dried at 60 °C and gathered for further characterization.

The morphology of the crystals was studied by scanning electron microscope (SEM) using JEOL JSM6300 model operating at 10kV. Photoluminescence (PL) experiments were performed in backscattering geometry using a He–Cd laser (325 nm) with an optical power of 30mW for excitation. The emitted light was analyzed by HR-4000 Ocean Optics USB spectrometer optimized for the UV–Visible range. For photoluminescence measurements, 0.05 g powder samples were pressed into pellets (10 mm diameter and 1 mm thickness) and then exposed to a 325 nm He-Cd laser. All measurements were carried out at room temperature. The structural characterization was performed by high resolution X-ray diffraction (XRD) using Rigaku Ultima IV diffractometer in the  $\theta$ – $2\theta$  configuration and using Cu K $\alpha$  radiation (1.54184 Å).

## RESULTS AND DISCUSSION

### Photo luminescence Spectra



a

FIGURE 1. (a) PL emission spectra of Ta<sub>2</sub>O<sub>5</sub>: Eu<sup>3+</sup> (2 mol %): Mg<sup>2+</sup> (5 mol%, 10 mol%, 15mol %)

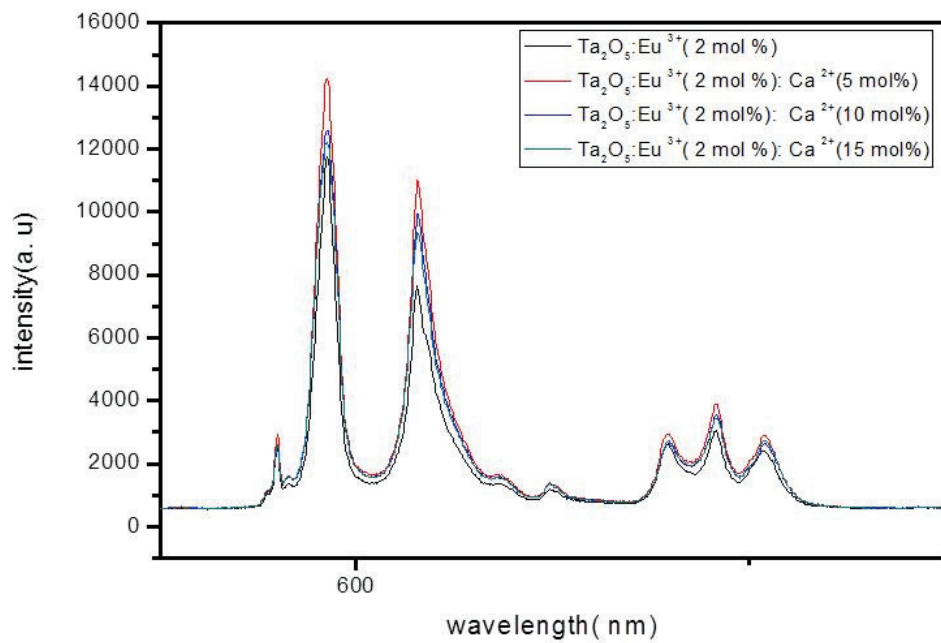


FIGURE 1. (b) PL emission spectra of Ta<sub>2</sub>O<sub>5</sub>: Eu<sup>3+</sup> (2 mol %): Ca<sup>2+</sup> (5 mol%, 10 mol%, 15mol %)

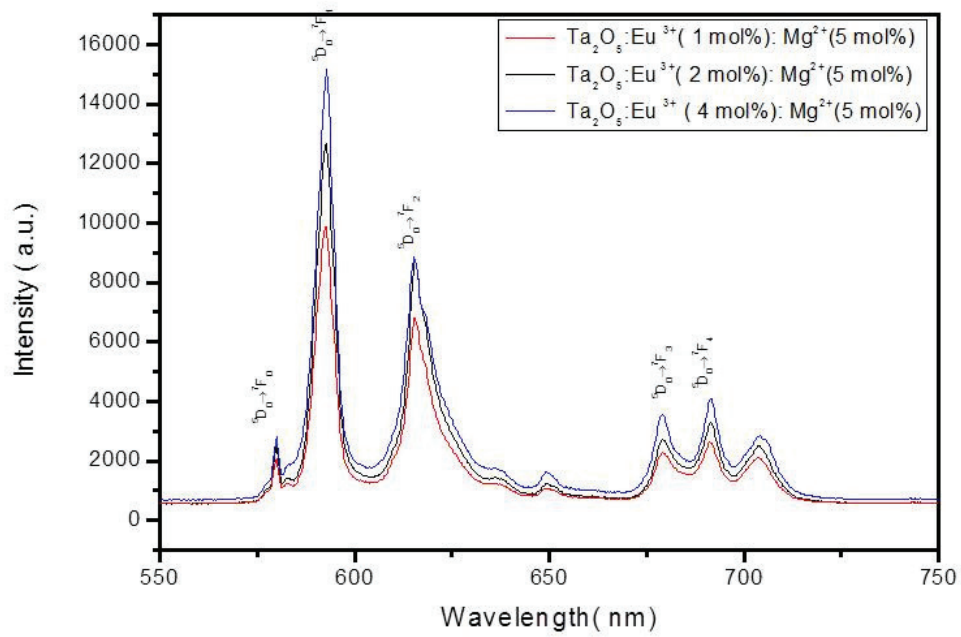


FIGURE 1. (c) PL emission spectra of Ta<sub>2</sub>O<sub>5</sub>: Eu<sup>3+</sup> (1, 2, 4 mol %): Mg<sup>2+</sup> (5mol%)

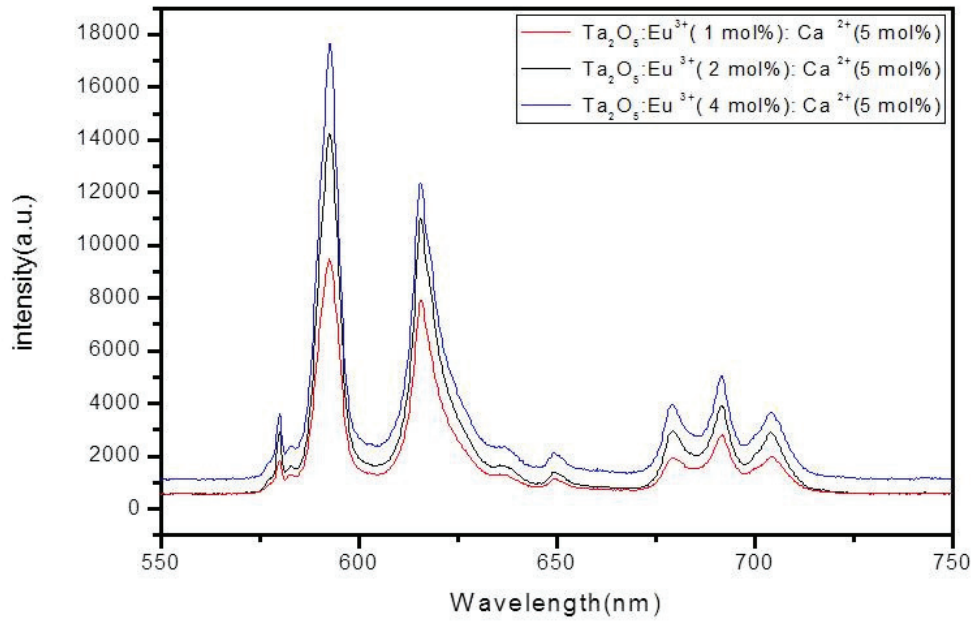


FIGURE 1. (d) PL emission spectra of Ta<sub>2</sub>O<sub>5</sub>: Eu<sup>3+</sup> (1, 2, 4 mol %): Ca<sup>2+</sup> (5 mol %)

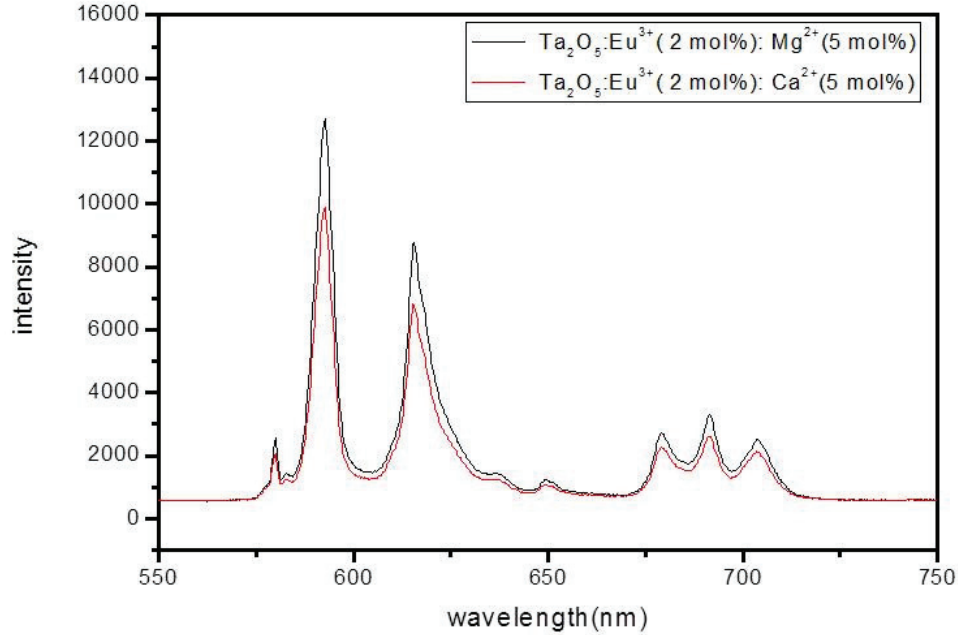


FIGURE 1. (e) Comparison of PL emission spectra of  $\text{Ta}_2\text{O}_5:\text{Eu}^{3+}$  (2 mol %):  $\text{Mg}^{2+}$  (5 mol %) and  $\text{Ta}_2\text{O}_5:\text{Eu}^{3+}$  (2 mol %):  $\text{Ca}^{2+}$  (5 mol %)

Luminescence spectra of  $\text{Ta}_2\text{O}_5$  doped with europium (III) ion and co-doped with  $\text{Mg}^{2+}$  or  $\text{Ca}^{2+}$  ions have been investigated. Figure 1 (a, b, c, d) represents the photoluminescence emission spectra of  $\text{Ta}_2\text{O}_5:\text{Eu}^{3+}$  phosphor with different concentrations of alkaline earth metal ions ( $\text{Mg}^{2+}$  and  $\text{Ca}^{2+}$ ). After incident excitation wavelength level, considerable radiative emission appears from the  $^5\text{D}_0$  metastable state to  $^7\text{F}_j$  ( $J = 0, 1, 2, 3, 4$ ) in the range of 550 nm to 720 nm. The emission spectra display bands at 580 nm, 592 nm, 615 nm, 679 nm and 691 nm in the visible region which are ascribed to the transition from  $^5\text{D}_0$  metastable state to lower lying  $^7\text{F}_0$ ,  $^7\text{F}_1$ ,  $^7\text{F}_2$ ,  $^7\text{F}_3$  and  $^7\text{F}_4$  states correspondingly. At the point when whatever other levels over the  $^5\text{D}_0$  are energized, there is speedy non radiative relaxation to the energized fluorescent level because of the small energy gaps between them and hence the same emission range is acquired [21]. It is clear from PL spectra (fig 1) that  $^5\text{D}_0 \rightarrow ^7\text{F}_1$  transition (magnetic dipole transition) at 592 nm is dominant over the  $^5\text{D}_0 \rightarrow ^7\text{F}_2$  (electric dipole transition) at 615 nm suggesting a higher occupancy of  $\text{Eu}^{3+}$  in a symmetric environment i.e.  $\text{Eu}^{3+}$  ions is located at crystallographic site with inversion centre. [22]. If the magnetic dipole transition  $^5\text{D}_0 \rightarrow ^7\text{F}_1$  having the highest intensity, then  $\text{Eu}^{3+}$  ions in host lattice occupies an inversion centre.  $^5\text{D}_0 \rightarrow ^7\text{F}_1$  transition is independent of the crystal field strength around  $\text{Eu}^{3+}$  ions. This transition could be utilized for the estimation of transition probabilities of different energized levels. The transition  $^5\text{D}_0 \rightarrow ^7\text{F}_j$  with  $J = 5$  and 6 are not observed as transition probabilities of these transitions are very weak.

It can be observed from photoluminescence spectra (Fig. 1a and 1 b) that, the luminescence intensity increases after the doping of  $\text{Mg}^{2+}$  or  $\text{Ca}^{2+}$  (5 mol %) but further increase of  $\text{Mg}^{2+}$  or  $\text{Ca}^{2+}$  concentration (10 mol % and 15 mol %), the luminescence intensity decreases. This might be due to concentration quenching. The increased in the luminescent intensity by the addition of  $\text{Mg}^{2+}$  or  $\text{Ca}^{2+}$  ion might be due to the vacancies which arises due to the charge difference between the lattice ion ( $\text{Ta}^{5+}$ ) and the co-dopant ion ( $\text{Mg}^{2+}$  or  $\text{Ca}^{2+}$ ). Thus, the doping of alkaline

earth metal ions ( $Mg^{2+}$  or  $Ca^{2+}$ ) up to 5 mol % enhanced the luminescence and it is favorable for luminescent applications.

PL plots (Fig. 1c & 1d) shows that the emission intensity of the samples continuously increases with increasing  $Eu^{+3}$  ion concentration. PL spectra (Fig 1 e) of  $Ta_2O_5: Eu^{+3}$  phosphor with  $Mg^{2+}$  as co-dopant have higher intensity than  $Ta_2O_5: Eu^{+3}$  phosphor with  $Ca^{2+}$ .

### XRD Measurement

The X ray powder diffraction (XRD) pattern of  $Ta_2O_5: Eu^{+3}$  with various concentrations of  $Mg^{2+}$  and  $Ca^{2+}$  alkaline earth metal oxides were shown in Fig 2 a and b. The peak width value ( $\beta$ ) is inversely proportional to crystallite size, as the crystallite sized gets smaller, the peak gets broader.

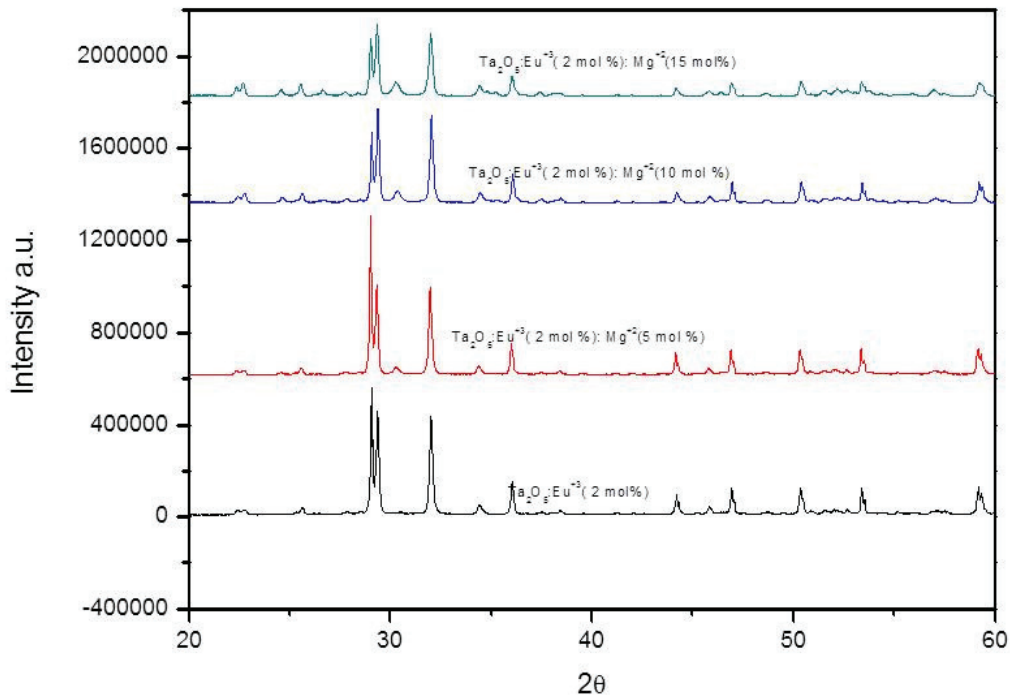


FIGURE2. (a) XRD pattern of  $Ta_2O_5: Eu^{+3}: Mg^{+2}$  sintered at  $800^\circ C$  for 2 hr.

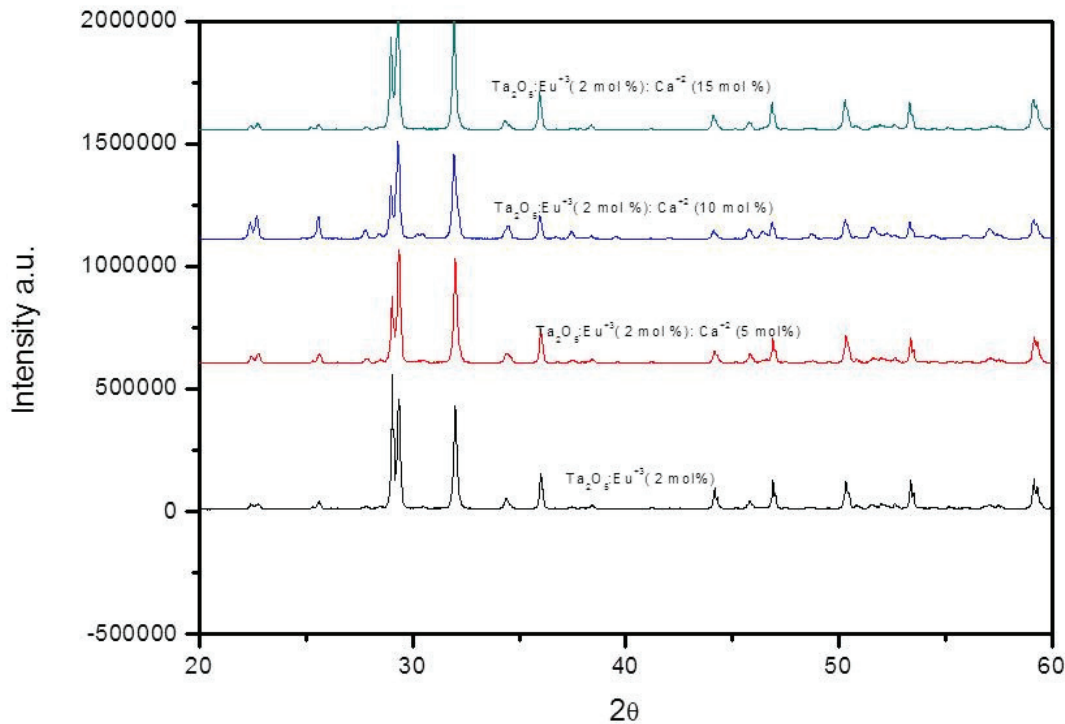


FIGURE2. (b) XRD pattern of Ta<sub>2</sub>O<sub>5</sub>: Eu<sup>3+</sup>: Ca<sup>2+</sup> sintered at 800°C for 2 hr.

The phosphor combined with KCl as a flux at the temperature of 800°C demonstrates the ideal crystallinity contrast compared to another salts. It is assessed that KCl as liquid salt will contribute to the dissolution and development of the crystal which may promote the solid state reaction. The measure of the particle has been figured from the full width half maxima of the extra ordinary peak using Debye Scherrer formula. Particle size of the sample in the range 0.3 μ to 4.0 μ is found. Formula used for calculation is

$$D = \frac{0.9\lambda}{\beta \cos\theta}$$

Here

D = particle size

B = Full width half maxima

λ = wavelength of x- ray source

θ = Angle of diffraction

The observed peaks in XRD pattern were found to be in agreement with JCPDS card no. 021-1199 and 025-0922. XRD data of samples confirm the formation of dual phase of Ta<sub>2</sub>O<sub>5</sub> phosphor, one phase is tetragonal and another one is orthorhombic. The absence of other phases regarding the dopants confirms the successful doping of Eu<sup>3+</sup> and Ca<sup>2+</sup> or Mg<sup>2+</sup> in the Ta<sub>2</sub>O<sub>5</sub> lattice.

### SEM Analysis

Figure 3 provides the typical SEM images of as prepared tantalum phosphor samples via molten method with good dispersion of granules. The most of the particles are hexagonal tablet shaped and highly distinguished. Some of the particles are Rod like shapes.

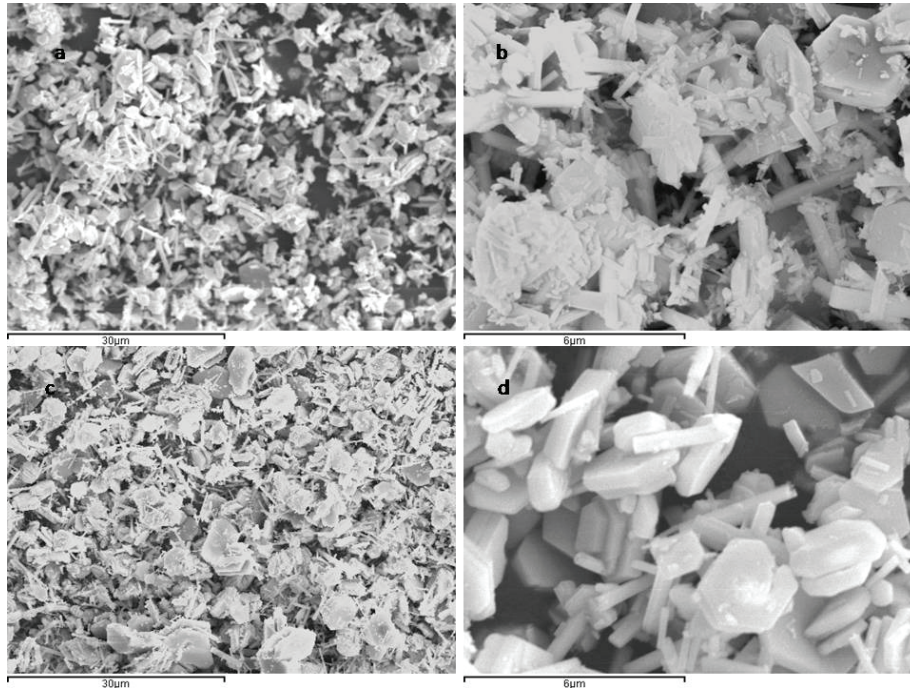


FIGURE3. SEM images of  $\text{Ta}_2\text{O}_5: \text{Eu}^{3+}: \text{Mg}^{2+}$  (a and b)  $\text{Ta}_2\text{O}_5: \text{Eu}^{3+}: \text{Ca}^{2+}$  (c and d)

### Raman Measurements

Unpolarized room-temperature Raman scattering experiments in backscattering geometry were performed using a HeNe laser (633 nm line) and Ar laser (528 nm line). The signal was collected by a Horiba Jobin Yvon Lab RAM HR microspectrometer equipped with a thermoelectrically-cooled multichannel CCD detector and a spectral resolution better than  $2 \text{ cm}^{-1}$ .

Comparing the annealed  $\text{Ta}_2\text{O}_5$  sample with the non-annealed, we did not observe any significant variation (Fig 4a).

The measurement performed with green laser (Ar line) presents bands that can be related to the luminescence of the sample. For this reason we decided to take all measures with the red laser (Fig. 4 b).

The rare earth doped samples show a quite different Raman spectrum than the  $\text{Ta}_2\text{O}_5$  taken commercially which is orthorhombic phase (Fig. a, c, d). At first we thought it might be luminescence, but as the measurements made with both red and green laser showed the same peaks, we have an indication that the peaks are Raman modes of the sample. In this case, heating of commercial  $\text{Ta}_2\text{O}_5$  with flux and doping ions and recrystallization of doped  $\text{Ta}_2\text{O}_5$  might have some change in material structure. This hypothesis also confirmed by X-ray diffraction measurements which shows the presence of two different  $\text{Ta}_2\text{O}_5$  phases i.e. tetragonal and another one is orthorhombic.

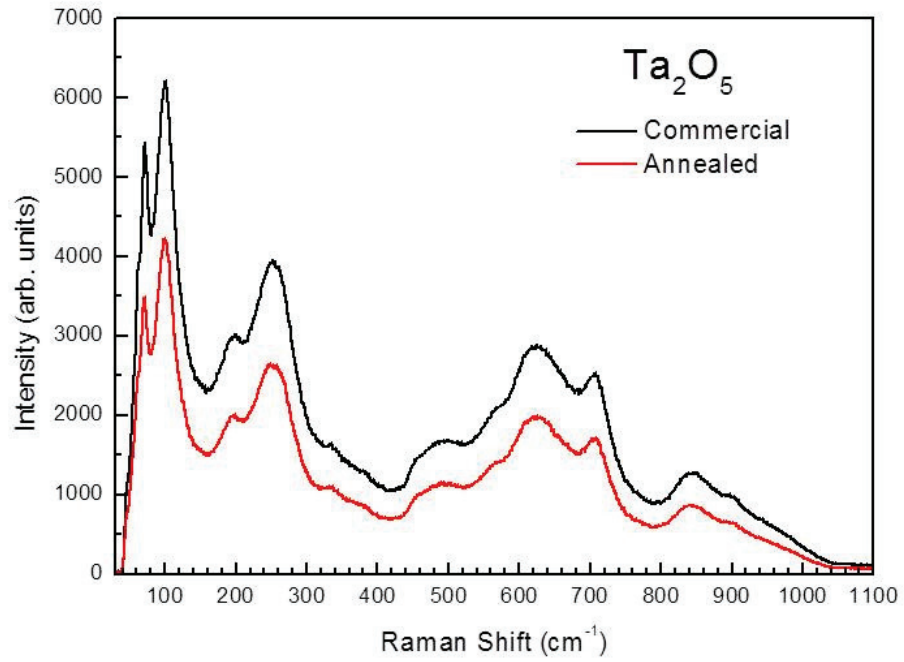


FIGURE4. (a) The Raman spectra of commercial samples

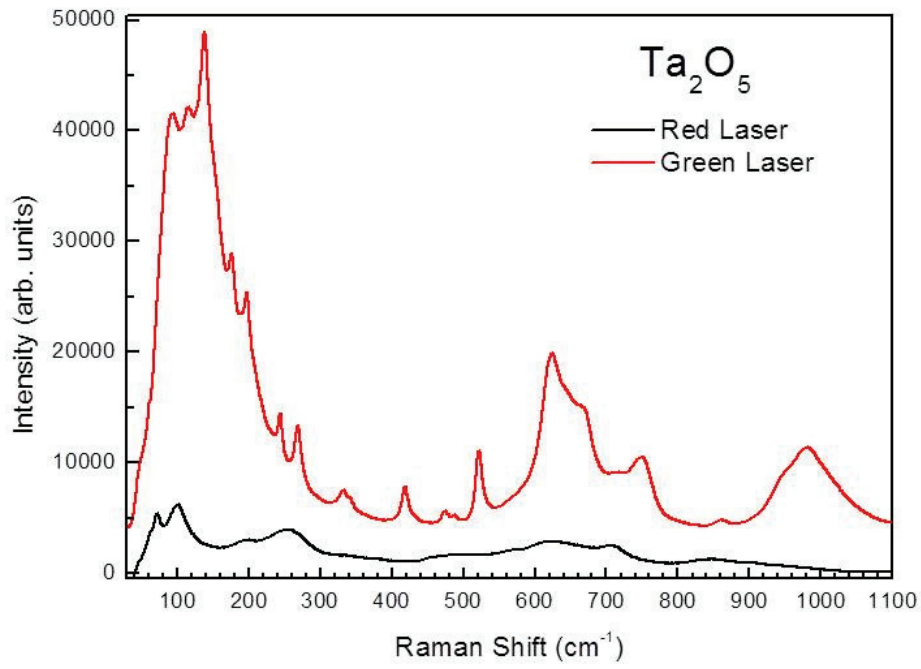


FIGURE4. (b) The Raman spectra of Ta<sub>2</sub>O<sub>5</sub> with different lasers

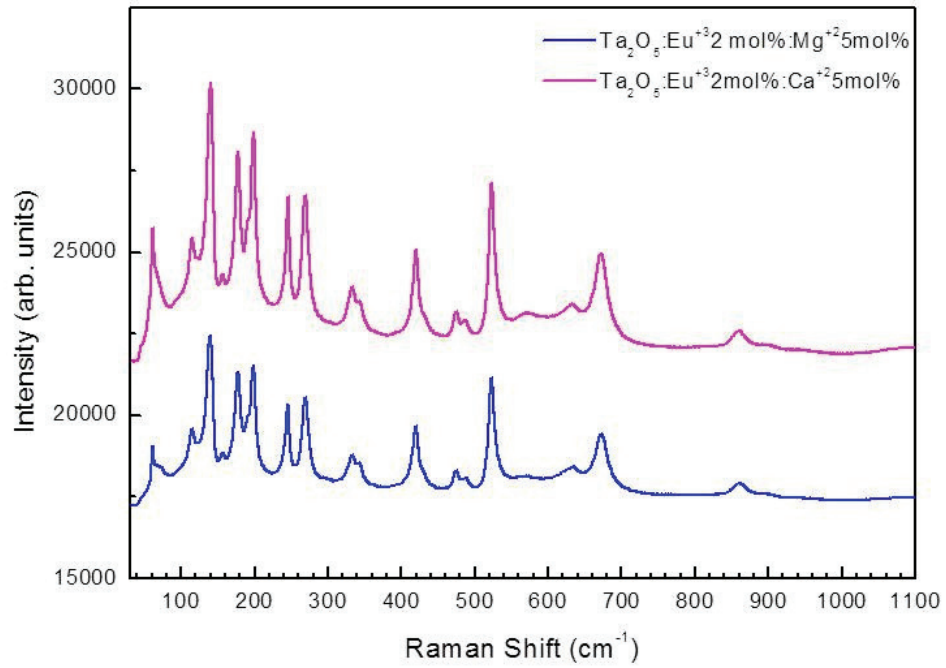


FIGURE4. (c) The Raman spectra of samples of Ta<sub>2</sub>O<sub>5</sub> doped with Eu<sup>+3</sup> and Mg<sup>+2</sup> or Ca<sup>+2</sup>

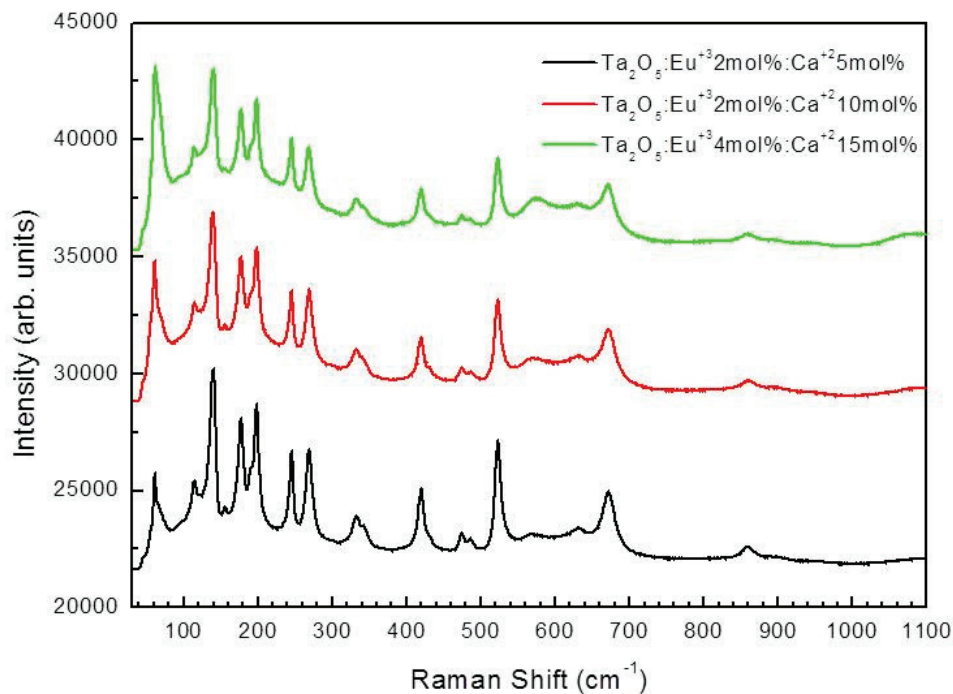


FIGURE4. (d) The Raman spectra of samples of  $\text{Ta}_2\text{O}_5$  doped with  $\text{Eu}^{+3}$  and  $\text{Mg}^{+2}$  or  $\text{Ca}^{2+}$

## CONCLUSIONS

In summary,  $\text{Ta}_2\text{O}_5: \text{Eu}^{3+}: \text{Ca}^{2+}$  or  $\text{Mg}^{2+}$  has been successfully prepared with KCl as flux via the molten salt method. The photo-luminescent properties of  $\text{Ta}_2\text{O}_5: \text{Eu}^{3+}: \text{Ca}^{2+}: \text{Mg}^{2+}$  shows the intense luminescence of  $\text{Eu}^{3+}$  which demonstrate that,  $\text{Ta}_2\text{O}_5$  is an efficient lattice for  $\text{Eu}^{3+}$ . The enhancement in luminescence is observed with the addition of  $\text{Mg}^{2+}$  or  $\text{Ca}^{2+}$ . XRD Pattern confirms the presence of the formation of dual phase of  $\text{Ta}_2\text{O}_5$  phosphor, one phase is tetragonal and another one is orthorhombic.

## ACKNOWLEDGMENT

This work was supported by the European Commission through Nano CIS project (FP7-PEOPLE-2010-IRSES ref. 269279).

## REFERENCES

1. L. Yi, Y. Hou, H. Zhao, D. He, Z. Xu, Y. Wang and X. Xu, *Displays* **21**, 147-149 (2000).
2. S. Shionoya, W. M. Yen, "Phosphor handbook", in *M. J. Weber (Ed.)*, (CRC press, Boca Raton, 1999).

3. U Rambabu, P. K Khanna, I. C Rao and S Buddhudu, *Mater. Letters* **34**, 269-274 (1998).
4. D. Vorkapic and T. Matsuoukas, *J. Am. Ceram. Society* **81**, 2815-2820 (1998).
5. U. Rambabu and S. Buddhudu, *Opt. Materials* **17**, 401-408 (2001).
6. M. P. Brown and K. Austin, *Appl. Phys. Letters* **85**, 2503-2504 (2004).
7. T. Monteiro, A. J. Neves, M. J. Soares, M. C. Carmo, M. Peres, E. Alves and E. Rita, *Appl. Phys. Letters* **87**, 192108-192110 (2005).
8. A. S. S. de Camargo, C. R. Ferrari, R. A. Silva, L. A. O. Nunes, A. C. Hernandez and J. P. Andreetta, *J. Luminescence* **128**, 223-226 (2008).
9. A. T. de Figueiredo, V. M. Longo, S. de Lazaro, V. R. Mastelaro, F. S. De Vicente, A. C. Hernandez, M. S. Li, J. A. Varela and E. Longo, *J. Luminescence* **126**, 403- (2007).
10. A. J Kenyon, *Prog. Quantum electron* **26**, 225-284 (2002).
11. P. S. Dobal, R. S. Katiyar, Y. Jiang, R. Guo and A. S. Bhalla, *J. Raman Spectroscopy* **31**, 1061-1065 (2000).
12. X. Xiao and B. Yan, *J. Alloy. Compounds* **456**, 447-451 (2008).
13. I. Arellano, M. Nazarov, C. C. Byeon, E. J. Popovici, H. Kim, H. C. Kang and D. Y. Noh, *Mater. Chem. Physics* **119**, 48-51 (2010).
14. T. K. Park, H. C. Ahn and S.Mho, *J. Korean Phys. Society* **52**, 431-434 (2008).
15. W. Liu, Q. Zhang, L. Ding, D. Sun, J. Luo and S. Yin, *J. Alloy Compound* **474**, 226-228 (2009).
16. E. C. Karsu, E. J. Popovici, A. Ege, M. Morar, E. Indrea, T. Karali and N. Can, *J. Luminescence* **131**, 1052-1057 (2011).
17. G. L. Brennecka, D. A. Payne, P. Sarin, J. M. Zuo, W. M. Kriven and H. Hellwig, *J. Am. Ceram. Society* **90**, 2947-2953 (2007).
18. H. Rigneault, F. Flory, S. Monneret, S. Robert and L. Roux, *Appl. Optics* **35**, 5005-5012 (1996).
19. B. Unal, C. Tai, D. P. Shepherd, J. S. Wilkinson, N. M. B. Perney, M. C. Netti and G. J. Parker, *Appl. Phys. Letters* **86**, 102-110 (2005).
20. C. Grivas and R. W. Eason, *J Phys. Condens. Matter* **20**, 264011- (2008).
21. B. D. Prasad Raju and C. M. Reddy, *Opt. Materials* **34**, 1251-1260 (2012).
22. K. Lee, B. Yong Yu, C. Pyun, S. Mho, *Solid State Communications* **122**, 485-488 (2002).